Flutter Prediction Based on Fluid-Structural Interactions of Wing with Winglet

K. M. Sridhar
Assistant Professor of Aero Dept
M.A.M School of Engineering

M. Prasanth
Dept .of Aero Eng
M.A.M School of Engineering

P. Palanisamy
Dept. of Aero Eng
M.A.M School of Engineering

B. Sajahan
Dept. of Aero Eng
M.A.M School of Engineering

Abstract:- **Aircraft components are naturally elastic which has its own natural frequency. When the source frequency is equal to objects natural frequency, the object may be tends to vibrate and deform. This may result in flutter. Flutter is an oscillatory instability occurs in airplane wing and control surfaces. The oscillatory motion of fluttering cantilever beam has both flexural and torsional component. The aircraft wing has infinitely many degrees of freedom due to cantilever beam structure. The main focus of this article is to predict the flutter of an aircraft wing with combination of winglet for different mach number and different altitude. Modelling of fluid and structural domain are required to solve FSI phenomena. The wing model has been analysed at certain constant altitude in subsonic range using optimization CFD and FEA tools. The deformation exist in a wing with winglet model caused by dynamic aeroelastic effects. The resulting structural deformation and stress variation corresponding to the flow are fully studied and validated with the help of numerical analysis.**

Keywords: Aeroelasticity, deformation, flutter, FSI, stress variation

1. INTRODUCTION

Wing are the sources for lift in an aircraft. Due to the aeroelastic characteristics and stress distribution of wing, it may deform. The aircraft performance may change or decrease due to this

deformation. In this article, the flutter predicted interms of deformation and stress distribution over a wing model. There are two ways to calculate fluid structural interaction i.e., strongly coupled fluid structural interaction and partly coupled fluid structural interaction [1].

1.1 PREDICTING THE EFFECTS OF AEROELASTICITY

The aeroelastic effect occurring on a wing with winglet model due to the flow separation is considered for present analysis. The aerodynamic force predictions and their influence is done using a three-dimensional Navier-Stroke model with fully coupled iterations to identify the physical phenomena. Once the flow field solutions are converged using CFD tool, then the flexural motion of the wing caused by the influence of aerodynamic forces will be computed using FEA tool. The algorithm for partly coupled fluid structural interaction analysis is presented in figure 1.The aerodynamic forces are solved by using flow field governing equations. The structural displacement are solved by using structural governing equations.

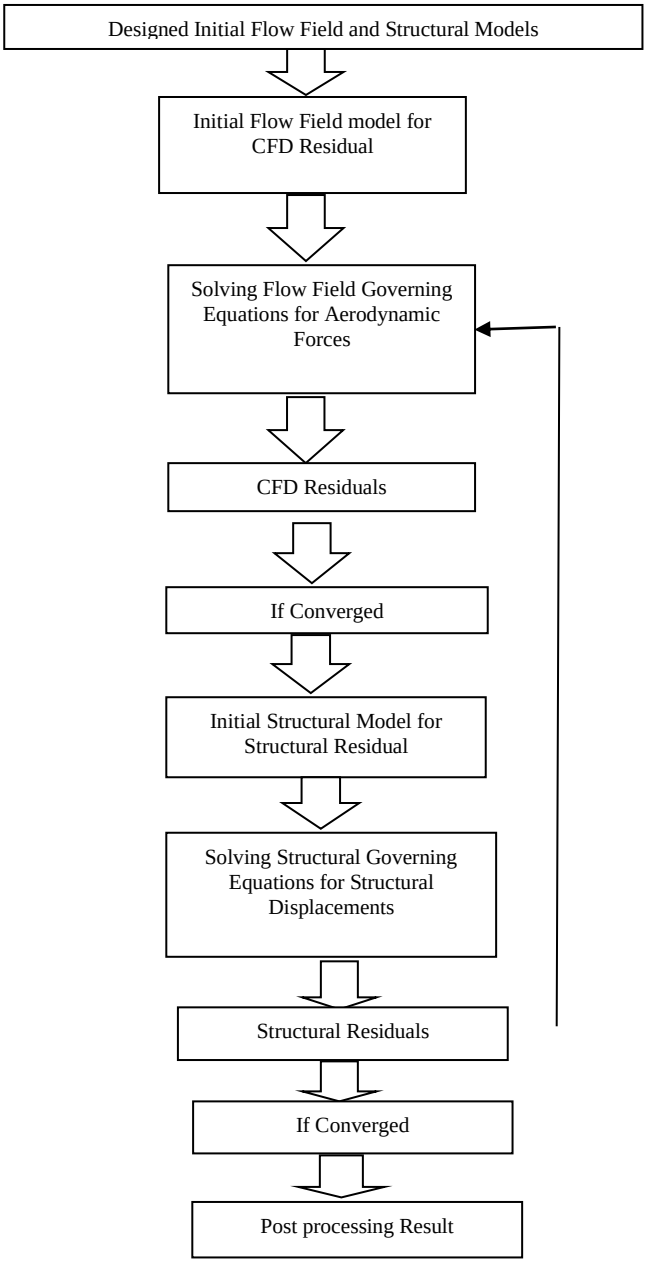

FIGURE 1: ALGORITHM FOR PARTLY COUPLED FOR FLUID STRUCTURAL INTERACTION ANALYSIS

2. PROBLEM DESCRIPTION

2.1 MODEL DESCRIPTION

Rectangular wing with 60º cant angle winglet is used for aeroelastic analysis. The airfoil used was a NACA 65_3218. The wing model were modelled using design software. NACA six series, NACA 65_3218 is used to model the rectangular wing with elliptical winglet. In NACA 65_3218 airfoil, the position of minimum pressure is 0.5, design lift coefficient is 0.2, range of lift coefficient is 0.3, maximum thickness is 18% at 39.9% chord and maximum camber is 1.1% at 50% chord. The specification of wing and winglet are shown in table 1 and 2.

TABLE 1: SPECIFICATION OF WING

SI. NO.	PARAMETERS OF MODEL	TYPES AND DIMENSIONS
1.	Wing type	Rectangular wing model
2.	Airfoil type	NACA 65_3218 airfoil
3.	Chord length	121mm
4.	Wing span length	660mm
5.	Semi-span length	330mm

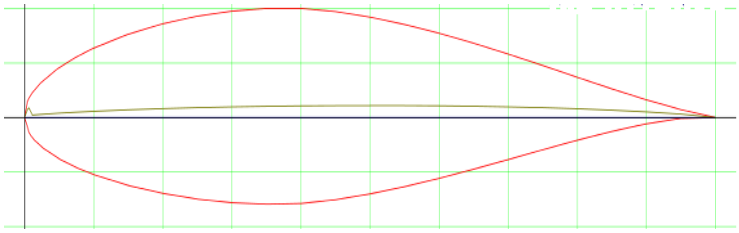

FIGURE 2: NACA 65_3218 AIRFOIL

TABLE 2: SPECIFICATION OF WINGLET

SI. NO.	PARAMETERS OF MODEL	TYPES AND DIMENSIONS
1.	Winglet type	Elliptical winglet
2.	Airfoil type	NACA 65_3218 airfoil
3.	Winglet root chord	121mm
4.	Winglet tip chord	60.5mm
5.	Angled height	55.1mm
6.	Vertical height	47.7mm
7.	Horizontal height	27.6mm
8.	Cant angle	60º

Using the specification which is tabulated in table I and II, the wing with winglet model is designed using modelling software. The designed wing model is shown in figure 3.

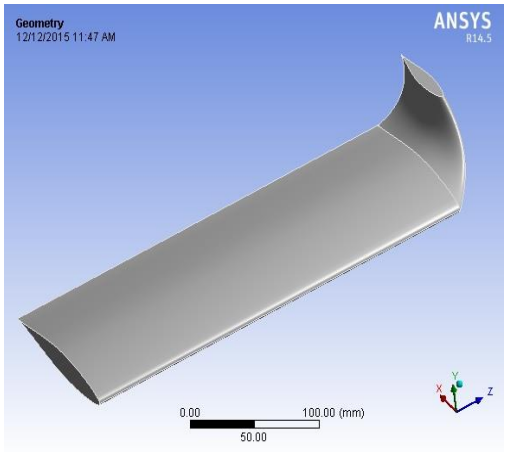

FIGURE 3: DESIGNED RECTANGULAR WING WITH ELLIPTICAL WINGLET MODEL IN 3D VIEW

A C-Domain control volume is used for flow field analysis. The wing with winglet model including the C-Domain Control Volume is depicted in figure 4. The control volume and the wing with winglet model are subtracted with each other. The total wing with winglet model area is immersed inside the control volume and one face of the wing model is attached with the side face of the control volume.

2.2 GRID GENERATION

A fine tetrahedron grid is generated for both the control volume and wing model as shown in figure 5. Tetrahedron grid is preferred for 3-D solid structures. Totally 178484 nodes and 703930 elements are generated for the control volume which is used for flow field analysis as shown in figure 4.

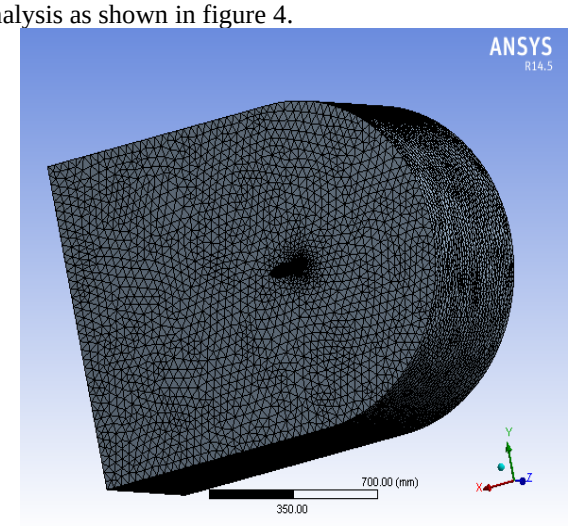

FIGURE 4: FINE GRID VIEW OF CONTROL VOLUME WITH THE WING STRUCTURE

Totally 199675 nodes and 126597 elements are generated for wing which is used for structural analysis as shown in figure 5.

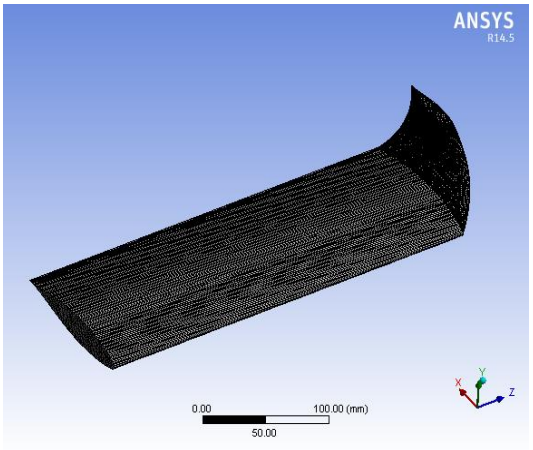

FIGURE 5: FINE GRID VIEW OF WING STRUCTURE

2.3 BOUNDARY CONDITION

In the control volume the face upright to the leading edge is considered as velocity inlet, the face just opposite to the velocity inlet is taken as pressure outlet and the remaining four faces of the
control volume are considered as symmetry faces. The upper and lower faces of the wing model are taken as fluid solid interface faces. The numerical
values of the boundary conditions are given as the International Standard Atmospheric (ISA) properties at 0km to 11km altitude which values are taken from reference 4. The velocity range is considered from 0.05 Mach to 0.75 Mach.

One face of the wing model attached to one face of the control volume and the symmetry face is converted into a fixed support for the structural analysis. The imported pressure load from the fluid flow solver is applied on the fluid- solid interface faces. Aluminium alloy is the material used on wing model design and its properties are shown in table 3.

TABLE 3: PROPERTIES OF MATERIAL

No	Variables	Properties of material
1	Material	Aluminium alloy
2	Young's Modulus	71GPa
3	Density	2770 kg/m3
4	Bulk Modulus	69.608GPa
5	Poisson's Ratio	0.33

3. RESULTS AND DISCUSSIONS

3.1 FUNDAMENTAL VIBRATION ANALYSIS

The fundamental vibrational analysis of wing model carried out using modal analysis software package. The vector contour of Mode Shape 4 is shown in figure 6.

TABLE 4: FIRST TEN VIBRATIONAL ANALYSIS DATA

SI. NO.	MODE SHAPE	FREQUENCY (Hz)
1.	1	106.84
2.	2	513.6
3.	3	651.08
4.	4	807.35
5.	5	1752.8
6.	6	2385.2
7.	7	2700.7
8.	8	3063.00
9.	9	3455.6
10.	10	4066.9

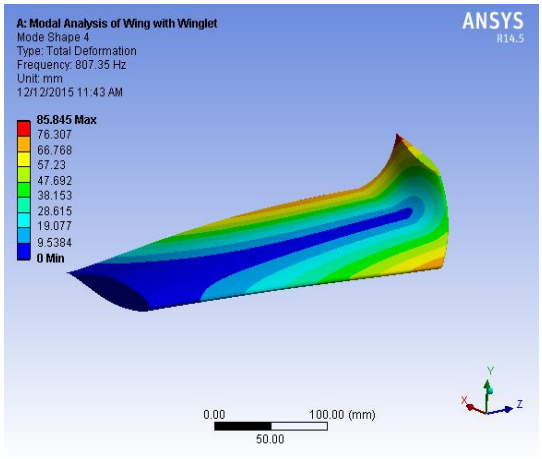

FIGURE 6: VECTOR CONTOUR OF MODE SHAPE 4

The main objective of modal analysis is to determine the dynamic characteristics of aircraft wing such as natural frequency, deformation and mode shapes. First ten vibrational analysis data are shown in table 4.

3.2 FLOW FIELD ANALYSIS

The flow field analysis are carried out for wing with winglet model at various mach numbers from 0.05 to 0.75 and at different altitude from 0km to 11km using Computational fluid dynamics tool.

Mach Number	Maximum Static Pressure (Pa)					
	Altitude h = 0km	Altitude h= 1km	Altitude h= 2km	Altitude h= 3km	Altitude h= 4km	Altitude h= 5km
0.05	1131.03	991.619	877.40	786.343	676.68	597.55
0.10	4580.09	4052.67	3584.2	3155.8	2859.2	2484.8
0.15	10352.30	9170.04	8116.2	7158.8	6349.3	5611.4
0.20	18263.50	16188.00	14487	12643	11196	9775.5
0.25	28542.70	25145.60	22275	21226	17320	15133
0.30	40454.20	35901.10	32087	28096	24820	21883
0.35	54589.90	48530.60	42925	38245	33521	29294
0.40	71616.20	62898.00	55683	49153	43495	37979
0.45	90245.10	79145.30	70611	62252	54688	47717
0.50	111435.0	97680.00	86310	76143	67308	58993
0.55	134176.0	118918.00	104160	91713	81113	71197
0.60	158012.0	139805.00	123350	108730	96147	84253
0.65	184838.0	163612.00	144400	127130	112480	98507
0.70	213681.0	189334.00	167110	147150	130190	113120
0.75	244942.0	218313.00	191430	168480	148990	129460

TABLE 5: MAXIMUM STATIC PRESSURE VS MACH NUMBERS FOR 0KM TO 5KM ALTITUDE

The maximum static pressure variation increases while mach number increases and decreases while altitude (h) increases as shown in figure 7. The minimum static pressure variation against mach number is shown in figure 9. The static pressure variation over the wing at 0.2 and 0.6 Mach number at 4km altitude is shown in figure 8 and 10 as a vector contour.

From this vector representation, it is evident that the maximum static pressure variation occurs at wing leading edge and minimum static pressure variation occurs at wing trailing edge. The pressure occurred at winglet region is less while compare with wing region as shown in figure 10 and 11. The computed maximum static pressure value against mach number is shown in table 5 and 6. The computed minimum static pressure value against mach number is shown in table 7 and 8.

Mach Number	Maximum Static Pressure (Pa)					
	Altitude h = 6km	Altitude h= 7km	Altitude h= 8km	Altitude h= 9km	Altitude h= 10km	Altitude h= 11km
0.05	517.94	450.05	388.53	336.45	288.36	246.66
0.10	2115.9	1886.3	1596.9	1377.9	1181.8	1010.4
0.15	4901.4	4184.2	3699.9	3132.0	2691.8	2304.2
0.20	8652.0	7478.2	6474.1	5591.6	4811.5	4119.6
0.25	13287	11586	10069	8707.5	7495.5	6446.0
0.30	19142	16536	14499	12439	10716	9201.8
0.35	25851	22528	19561	16773	14461	12415
0.40	33221	28962	25152	21932	18747	16086
0.45	42089	36382	31878	27349	23549	20210
0.50	51233	44634	39077	33534	28902	24780
0.55	62263	54274	47145	40489	34763	29835
0.60	73634	64187	55770	48243	41302	35430
0.65	85994	74917	65049	56270	48500	41354
0.70	98941	86484	75075	64951	55714	47769
0.75	113690	98684	85829	74046	63750	54629

TABLE 6: MAXIMUM STATIC PRESSURE VS MACH NUMBERS FOR 6KM TO 11KM ALTITUDE

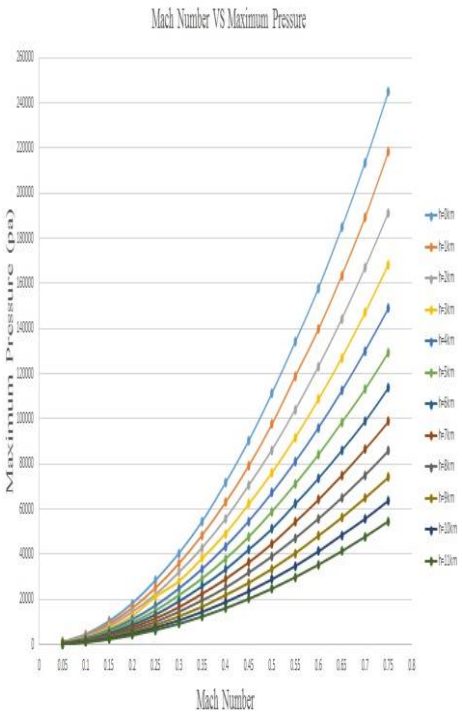

FIGURE 7: MAXIMUM PRESSURE VARIATION ABOUT MACH NUMBER AT 0KM TO 11KM ALTITUDE

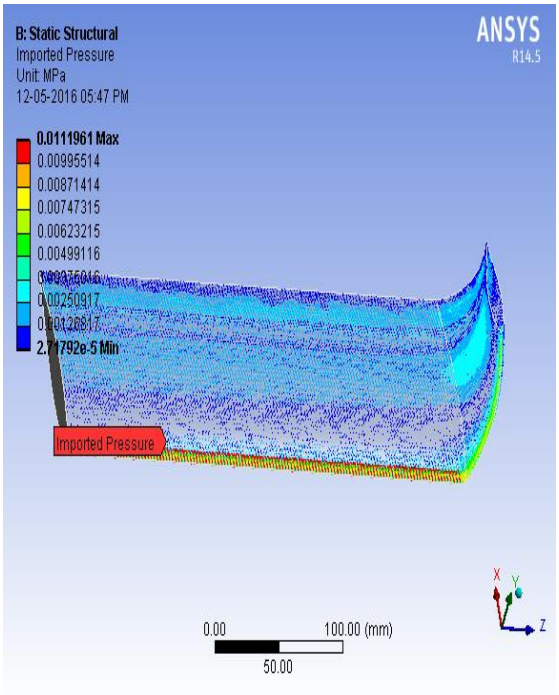

FIGURE 8: COMPUTED STATIC PRESSURE VARIATION AT 0.2 MACH NUMBER AT 4KM ALTITUDE

ach Number	Minimum Static Pressure (Pa)					
	h = 0km	h= 1km	h= 2km	h= 3km	h= 4km	h= 5km
0.05	2.6261 6	2.3985 5	2.1787 0	1.8895	1.7551	1.5694
0.10	10.692 0	9.6941 5	8.5818	6.6773	7.3119	5.8982
0.15	19.453 2	17.520 8	15.991	15.36	15.459	12.880
0.20	37.349 4	35.743 1	26.447	27.627	27.179	19.406
0.25	52.998 5	49.072 0	44.845	45.723	45.415	29.455
0.30	68.678 0	63.391 6	58.942	49.057	62.412	45.306
0.35	88.147 2	89.423 1	75.806	69.473	80.699	48.374
0.40	127.96 1	99.825 9	93.983	88.543	102.55	60.474
0.45	111.22 3	128.20 8	116.56	102.04	128.24	87.783
0.50	207.65 6	150.89 0	122.6	132.40	146.72	108.91
0.55	236.42 6	233.57 3	206.31	116.83	140.44	126.55
0.60	179.73 4	177.51 6	221.45	211.13	158.78	141.10
0.65	237.93 4	195.09 5	175.22	231.85	135.80	124.74
0.70	310.69 4	208.15 3	246.60	175.93	252.72	210.99
0.75	371.29 7	314.84 4	218.78	249.19	264.24	246.61

TABLE 7: MINIMUM STATIC PRESSURE VS MACH NUMBERS FOR 0KM TO 5KM ALTITUDE

Mach Number	Minimum Static Pressure (Pa)					
	h = 6km	h= 7km	h= 8km	h= 9km	h= 10km	h= 11km
0.05	1.4678	1.2543	1.0382	0.9288 6	0.9004 6	0.83003
0.10	4.9476	4.7553	4.7218	4.0647 0	3.4839 0	2.97210
0.15	11.776	10.285	9.3470	8.1781 0	7.2082 0	6.24590
0.20	22.837	18.727	14.422	12.683	11.254 0	10.1430
0.25	25.80 4	26.00 2	22.55 3	20.06 1	18.89 40	14.68 60
0.30	35.75 8	31.88 7	36.30 2	31.57 6	28.48 60	22.53 00
0.35	48.12 4	40.80 9	36.35 5	38.44 4	37.64 80	32.41 90
0.40	53.41 0	53.97 2	55.57 6	40.63 1	43.09 80	40.65 20
0.45	80.55 6	58.98 2	53.64 6	65.95 5	58.31 70	47.35 40
0.50	78.18 6	69.41 9	64.57 9	77.36 5	68.73 40	60.39 10
0.55	117.8 6	100.3 0	79.36 5	74.84 4	81.76 50	70.63 00
0.60	129.6 6	115.0 8	96.85 3	78.61 6	86.48 70	82.95 10
0.65	145.6 5	129.8 1	108.8 6	88.21 3	79.80 70	98.30 50
0.70	123.2 6	135.8 3	117.3 2	96.14 8	126.6 7	110.4 3
0.75	184.6 3	126.0 6	127.7 8	123.2 5	143.6 9	122.2 3

TABLE 8: MINIMUM STATIC PRESSURE VS MACH NUMBERS FOR 6KM TO 11KM ALTITUDE

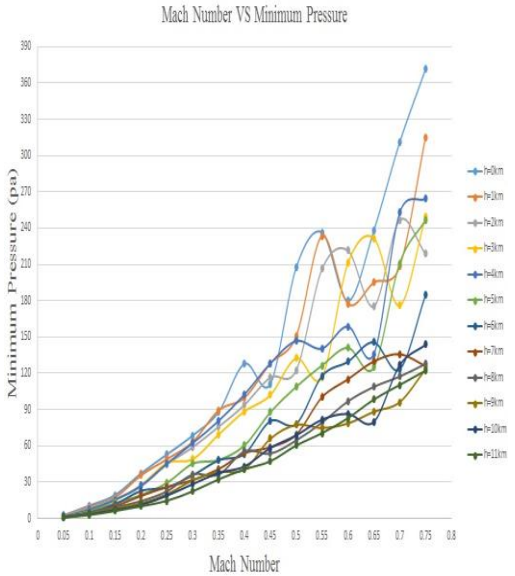

FIGURE 9: MINIMUM PRESSURE VARIATION ABOUT MACH NUMBER AT 0KM TO 11KM ALTITUDE

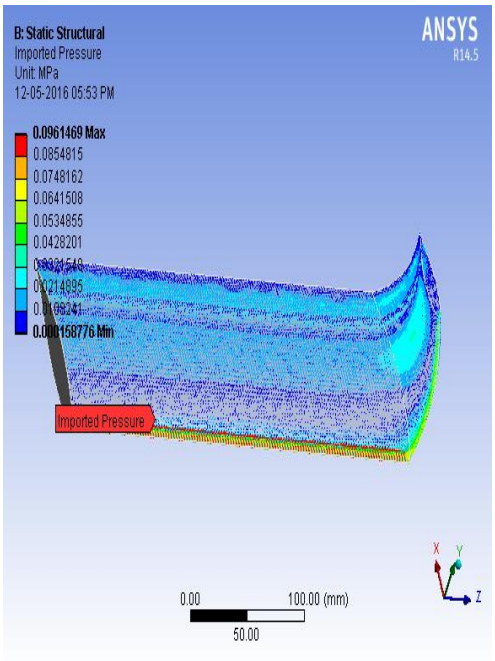

FIGURE 10: COMPUTED STATIC PRESSURE VARIATION AT 0.6 MACH NUMBER AT 4KM ALTITUDE

3.3 STRUCTURAL ANALYSIS

The total deformation and the equivalent Von- Mises stress distributions of the wing with winglet model are computed using Finite Element Analysis tool. The computed pressure load imported over wing with winglet model as shown in figure 8 and 10.

TABLE 9: EQUIVALENT VON – MISES MAXIMUM STRESS VS MACH NUMBERS FOR 0KM TO 5KM ALTITUDE

Mach Number	Equivalent Von - Mises Maximum Stress (Pa)					
	h = 0km	h= 1km	h= 2km	h= 3km	h= 4km	h= 5km
0.05	147600	122500	107150	98979	83749	72039
0.10	585780	515680	453330	394440	385790	328490
0.15	1383600	1209800	1061700	931680	913050	769740
0.20	2629100	2297900	2135000	1786000	1655400	1341000
0.25	4357300	3723400	3233300	3232900	2631100	2184500
0.30	6172200	5432400	4966800	4180500	3812200	3357300
0.35	8495500	7487300	6612800	6011100	5243300	4432400
0.40	11459000	9948100	8749800	7672100	6893700	5876500
0.45	14552000	12630000	11434000	10079000	8763600	7529700
0.50	17990000	15627000	13823000	12187000	10856000	9616700
0.55	21898000	19454000	16874000	14832000	13198000	11713000
0.60	25581000	22738000	20134000	17841000	15745000	13998000
0.65	30279000	26871000	23772000	21000000	18639000	16490000
0.70	35210000	31410000	27772000	24568000	21490000	18920000
0.75	40498000	36370000	31971000	28190000	24823000	21826000

The equivalent Von - Mises stress variation caused by the pressure load acting on the wing at the inlet velocity of 0.2 and 0.6 Mach at 4km altitude is illustrated in figure 12 and 114. The maximum stress variations are tabulated which is shown in table 9 and 10 and minimum stress variations are tabulated which is shown in table 11 and 12. The maximum and minimum equivalent Von – Mises Stress variation increase while Mach number increases and also decreases while altitude increases as shown in figure 11 and 13.

Mach Number	Equivalent Von - Mises Maximum Stress (Pa)					
	h = 6km	h= 7km	h= 8km	h= 9km	h= 10km	h= 11km
0.05	60944	52277	44329	37964	32008	26838
0.10	260750	248790	195270	167090	142910	121680
0.15	671150	535960	502440	395620	337310	288480
0.20	1244200	994660	854680	733060	626300	533630
0.25	1882600	1630000	1403100	1206600	1029000	864720
0.30	2924100	2412400	2185500	1787300	1530800	1297400
0.35	4025700	3496000	3018700	2487500	2129900	1811700
0.40	5112800	4431100	3825000	3435400	2821000	2404600
0.45	6752800	5675000	5078900	4214600	3619400	3086300
0.50	8161500	7084300	6302600	5265900	4506100	3851000
0.55	10206000	8854900	7657600	6416600	5502900	4686500
0.60	12196000	10593000	9175400	7913800	6591000	5619400
0.65	14392000	12519000	10853000	9283400	8002300	6658500
0.70	16435000	14579000	12638000	10871000	9103800	7768000
0.75	19341000	16470000	14547000	12250000	10526000	8960700

TABLE 10: EQUIVALENT VON - MISES MAXIMUM STRESS VS MACH NUMBERS FOR 6KM TO 11KM ALTITUDE

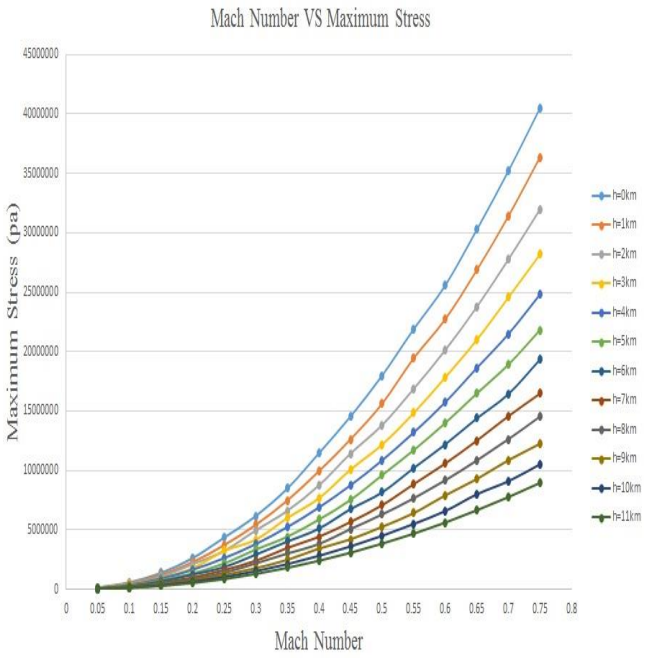

FIGURE 11: MAXIMUM STRESS VARIATION ABOUT MACH NUMBER AT 0KM TO 11KM ALTITUDE

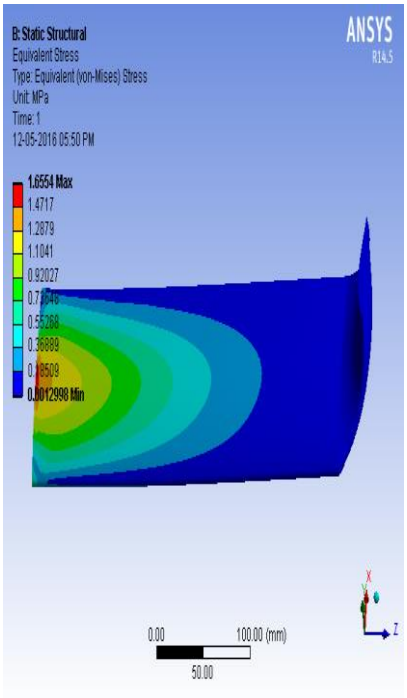

FIGURE 12: COMPUTED EQUIVALENT VON - MISES STRESS VARIATION AT 0.2 MACH NUMBER AT 4KM ALTITUDE

Mach Number	Equivalent Von - Mises Minimum Stress (Pa)					
	h = 0km	h= 1km	h= 2km	h= 3km	h= 4km	h= 5km
0.05	90.017	69.613	58.953	61.813	44.476	34.107
0.10	372.77	326.01	283.57	243.30	262.79	212.76
0.15	939.64	805.10	699.28	606.32	677.10	522.19
0.20	1926.6	1659.4	1642.5	1248.2	1299.8	902.08
0.25	3465.1	2792.6	2393.8	2541.8	2115.0	1552.3
0.30	4743.6	4145.6	3974	3150.1	3007.6	2642.1
0.35	6574.6	5767.0	5093	4766.3	4014.8	3362.7
0.40	8877.8	7758.5	6824.4	5952.8	5170.9	4517.4
0.45	11186.0	9864.1	8705.2	7655.7	6455.0	5850.8
0.50	13813.0	12203	10831	9598.3	7911.1	7257.9
0.55	16657.0	14692	13155	11635	9552.2	8679.2
0.60	19720.0	17531	15576	13815	11375	10243
0.65	23185.0	20585	18266	16157	13292	11976
0.70	26979.0	23935	21195	18713	15368	14503
0.75	30940.0	26964	24305	21456	17712	16607

TABLE 11: EQUIVALENT VON – MISES MINIMUM STRESS VS MACH NUMBERS FOR 0KM TO 5KM ALTITUDE

MACH NUMBER	**EQUIVALENT VON - MISES MINIMUM STRESS (PA)**					
	h = 6km	h= 7km	h= 8km	h= 9km	h= 10km	h= 11km
0.05	27.483	22.632	18.121	14.617	11.356	9.1446
0.10	163.91	162.27	128.53	109.14	87.708	70.593
0.15	449.57	339.42	333.94	251.65	216.07	188.50
0.20	892.36	634.10	552.60	471.25	400.90	341.09
0.25	1324.2	1124.6	949.73	803.48	677.60	562.41
0.30	2287.1	1745.1	1650.9	1244.9	1047.7	869.08
0.35	3183.7	2750.2	2335.0	1795.4	1509.3	1260.6
0.40	3910.1	3368.3	2887.9	2682.4	2061.8	1723.7
0.45	5247.4	4359.5	3999.8	3196.0	2693.8	2259.0
0.50	6355.7	5490.8	4878.5	4030.6	3428.2	2875.5
0.55	7614.3	6660.3	5814.3	4954.6	4218.3	3564.4
0.60	8966.0	7836.6	6837.9	5928.1	5098.5	4314.1
0.65	10434	9109.6	7932.3	6903.3	5981.9	5135.6
0.70	12699	10478	9123.0	7930.6	7081.4	6016.9
0.75	13797	12679	10392	9535.6	8207.3	6958.9

TABLE 12: EQUIVALENT VON – MISES MINIMUM STRESS VS MACH NUMBERS FOR 6KM TO 11KM ALTITUDE

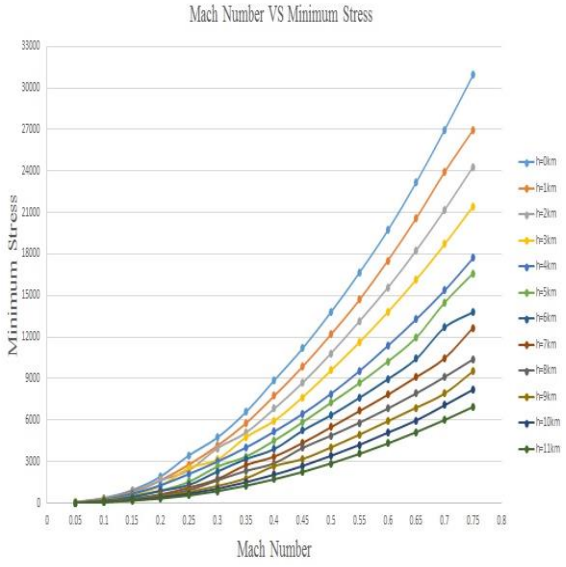

FIGURE 13: MINIMUM STRESS VARIATION ABOUT MACH NUMBER AT 0KM TO 11KM ALTITUDE

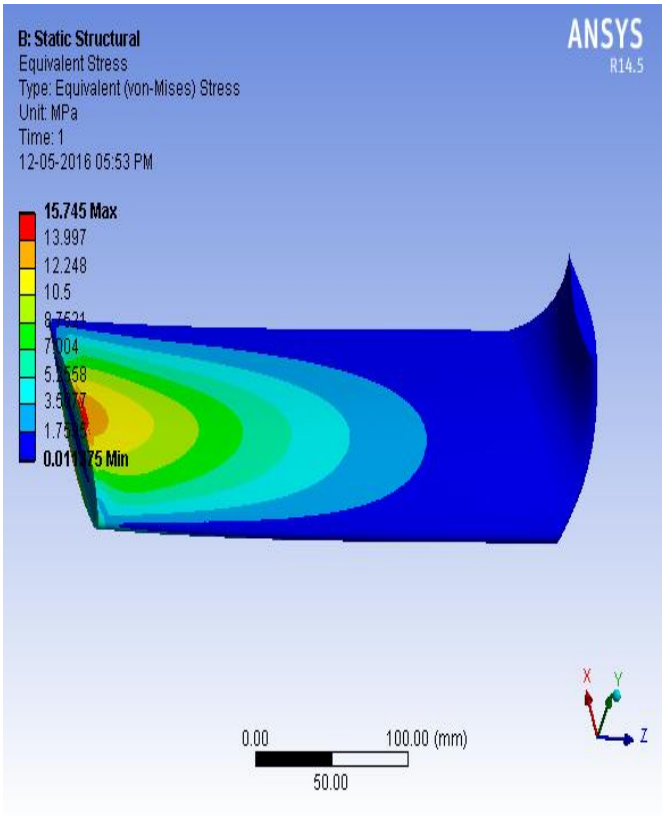

FIGURE 14: COMPUTED EQUIVALENT VON - MISES STRESS VARIATION AT 0.6 MACH NUMBER AT 4KM ALTITUDE

The total deformation distribution produced on the wing because of the pressure load acting on it (0.2 and 0.6 Mach number) is shown in figure 16 and 17. The total deformation value increases gradually from the wing root to winglet tip. The maximum deformation occurs at trailing edge wing tip to winglet tip. The wing for various velocity inlet conditions at different altitude, deformations values are computed as illustrated and tabulated in figure 15 and table 13 and 14.

Mach Number	Total Deformation (mm)					
	h = 0km	h= 1km	h= 2km	h= 3km	h= 4km	h= 5km
0.05	0.0056263	0.0045788	0.003996	0.0037463	0.0031535	0.0026795
0.10	0.022403	0.019694	0.017287	0.015014	0.015093	0.012691
0.15	0.053540	0.046699	0.040948	0.035907	0.036084	0.030038
0.20	0.103150	0.089932	0.084301	0.069839	0.065716	0.052248
0.25	0.173050	0.146870	0.127160	0.128300	0.104850	0.085731
0.30	0.244610	0.214980	0.197700	0.165030	0.152270	0.133400
0.35	0.337480	0.297210	0.262370	0.239730	0.209860	0.175390
0.40	0.458190	0.396140	0.348220	0.304990	0.276350	0.233280
0.45	0.582010	0.503360	0.457200	0.403050	0.353000	0.299780
0.50	0.7202	0.6231	0.5516	0.4866	0.4362	0.3844

	70	600	20	100	500	800
0.55	0.876260	0.778500	0.673410	0.592150	0.530550	0.468730
0.60	1.019000	0.905680	0.802430	0.711810	0.632790	0.560120
0.65	1.206500	1.070400	0.947460	0.837120	0.748500	0.659690
0.70	1.404200	1.252300	1.107100	0.979050	0.864130	0.754670
0.75	1.615700	1.456400	1.274400	1.123700	0.997200	0.870030

TABLE 13: TOTAL DEFORMATION VS MACH NUMBERS FOR 0KM TO 5KM ALTITUDE

Mach Number	Total Deformation (mm)					
	h = 6km	h= 7km	h= 8km	h= 9km	h= 10km	h= 11km
0.05	0.0022583	0.0019287	0.0016288	0.0013951	0.0011697	0.0009759 4
0.10	0.0098858	0.0095986	0.0073932	0.0063134	0.0053887	0.0045806 0
0.15	0.0261630	0.0205900	0.0195570	0.0151490	0.0128930	0.0110200 0
0.20	0.0489350	0.0385670	0.0330790	0.0283370	0.0241800	0.0205710 0
0.25	0.0738020	0.0638350	0.0548700	0.0471340	0.0401410	0.0336070 0
0.30	0.1161000	0.0949610	0.0866140	0.0702040	0.0600750	0.0508130 0
0.35	0.1602500	0.1390900	0.1200000	0.0981180	0.0839270	0.0713040 0
0.40	0.2027900	0.1755900	0.1514300	0.1368100	0.1115100	0.0949500 0
0.45	0.2697100	0.2255100	0.2026600	0.1671600	0.1434700	0.1222200 0
0.50	0.3253500	0.2822300	0.2516700	0.2094100	0.1790000	0.1528900 0
0.55	0.4083600	0.3542800	0.3062700	0.2557600	0.2190600	0.1863300 0
0.60	0.4880400	0.4238300	0.3670000	0.3164500	0.2629900	0.2239600 0
0.65	0.5758600	0.5008000	0.4339600	0.3714600	0.3198200	0.2656200 0
0.70	0.6564800	0.5832600	0.5054100	0.4346900	0.3634100	0.3100200 0
0.75	0.7733500	0.6581000	0.5819300	0.4894000	0.4202500	0.3576400 0

TABLE 14: TOTAL DEFORMATION VS MACH NUMBERS FOR 6KM TO 11KM ALTITUDE

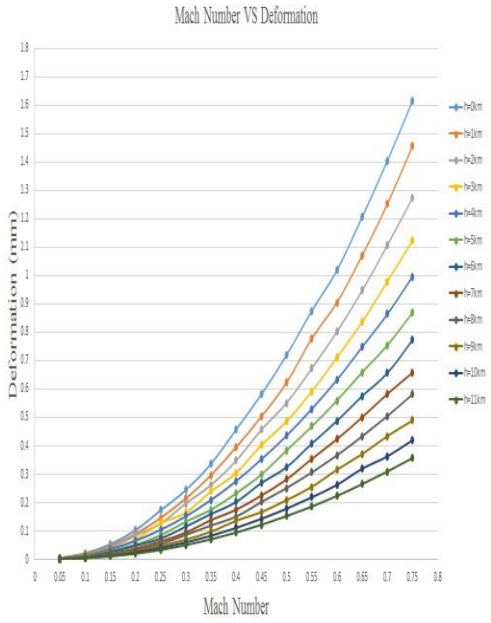

FIGURE 15: TOTAL DEFORMATION ABOUT MACH NUMBER AT 0KM TO 11KM ALTITUDE

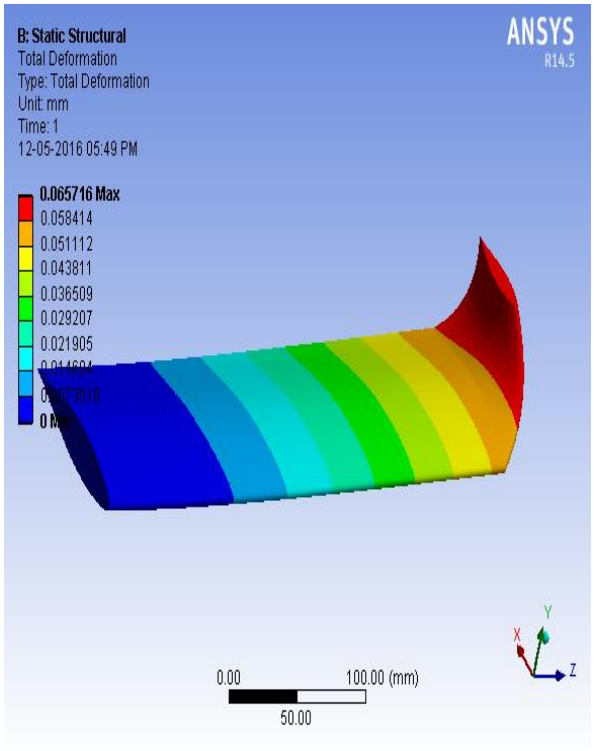

FIGURE 16: TOTAL DEFORMATION CONTOUR AT 0.2 MACH NUMBER AT 4KM ALTITUDE

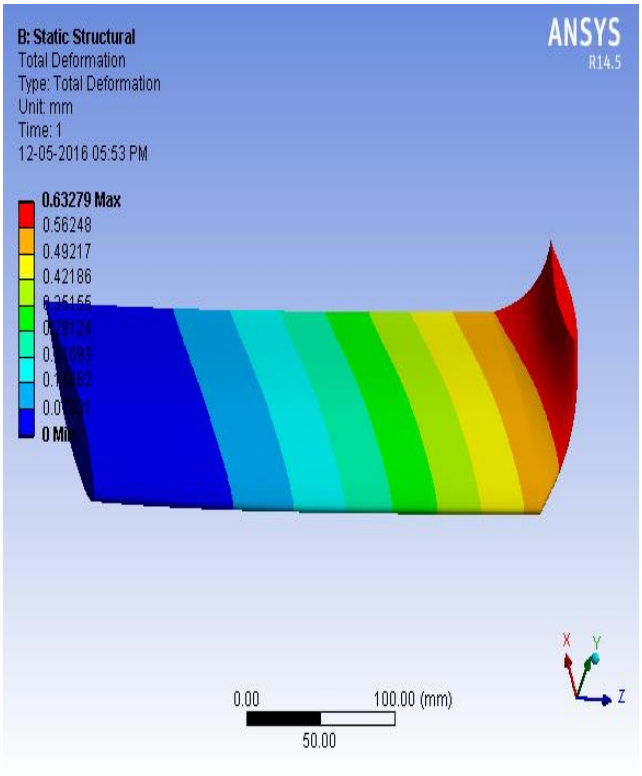

FIGURE 17: TOTAL DEFORMATION CONTOUR AT 0.6 MACH NUMBER AT 4KM ALTITUDE

4. CONCLUSION

The considered rectangular wing with winglet model is kept at 0º Angle of Attack throughout the analysis. Therefore, the pressure distributions obtained for the subsonic Mach numbers from 0.05 to 0.75 at different altitude are verified with the available historical data. The results are fully agreed with the data exist in the NACA report and verified with the fifteen inlet velocity conditions. From the results and contours, it is identified that the non-linear aeroelastic effects in the both incompressible and compressible subsonic velocities are negligible. The methodology used in this article can be implemented for Taper, Swept back and Delta wings with different wingtips with high subsonic Mach numbers to study the aeroelastic nature of such designs.

REFERENCES

[1] C.Bibin, Micheal Johnson Selvaraj and S.Sanju (2012), Flutter analysing over an aircraft wing during cruise speed, *Elsevier. Procedia Engineering* 38 (2012) 1950 – 1961.

[2] Daniella E. Raveh (2005), Computational-fluid-dynamics-based aeroelastic analysis and structural design optimization—a researcher's perspective, *Elsevier Computer Methods in Applied Mechanic and Engineering*. 194 (2005) 3453–3471.

[3] H. Haddadpour, R.D. Firouz-Abadi (2006), Evaluation of quasi-steady aerodynamic modeling for flutter prediction of aircraft wings in incompressible flow, *Elsevier. Thin-Walled Structures* 44 (2006) 931–936.

[4] John D Anderson Jr, Fundamentals of Aeronautics, *McGraw Hill companies*, fourth edition.

[5] John W. Edwards, Charles V. Spain, Donald F. Keller, and Robert W. Moses (2009), Transport Wing Flutter Model

Transonic Limit Cycle Oscillation Test, *Journal of Aircraft* Vol. 46, No. 4, July–August 2009.

[6] Justin W. Jaworski and Earl H. Dowell (2009), Comparison of Theoretical Structural Models with Experiment for a High-Aspect-Ratio Aeroelastic Wing, *Journal of Aircraft* Vol. 46, No. 2, March–April 2009.

[7] Nikhil A. Khadse and Prof. S. R. Zaweri (2015), Modal Analysis of Aircraft Wing using Ansys Workbench Software Package, *International Journal of Engineering Research & Technology (IJERT)* ISSN: 2278-0181 Vol. 4 Issue 07, July-2015.

[8] Seong Hwan Moon, Seung Jo Kim (2003), Suppression of nonlinear composite panel flutter with active/passive hybrid piezoelectric networks using finite element method, *Elsevier. Composite Structures* 59 (2003) 525–533.

[9] T.H.G.Megson, Aircraft structures for engineering students, *Edward Arnold Publisher limited*, ISBN : 0713133937

[10] Xiangying Chen, Ge-Cheng Zha and Ming-Ta Yang (2007), Numerical simulation of 3-D wing flutter with fully coupled fluid–structural interaction, *Elsevier. Computers & Fluids* 36 (2007) 856–867.

[11] Y.C,Fung, An introduction to aeroelasticity, *Dower publications*, Inc, Newyork.

[12] ZHAO Yong hui, HU Hai yan (2005), Structural Modeling and Aeroelastic Analysis of High Aspect Ratio Composite Wings, *Chinese Journal of Aeronautics*, Vol. 18 No. 1, February 2005.